RECENT RESULTS FROM P-BAND SIGNALS OF OPPORTUNITY RECEIVER DEPLOYED ON A MULTI-COPTER UAS PLATFORM

Mehmet Kurum⁽¹⁾, Preston Peranich⁽²⁾, Md Abdus Shahid Rafi⁽¹⁾, Md Mehedi Farhad⁽¹⁾, and Dylan Boyd⁽¹⁾

(1) Mississippi State University, Department of Electrical and Computer Engineering,
 Mississippi State, MS, 36792, USA
(2) Johns Hopkins University, Applied Physics Laboratory,
 Laurel, MD, 20723 USA

ABSTRACT

P-band Signals of Opportunity (SoOp) is an innovative technique that shows promise for many earth observation applications including remote sensing of root-zone soil moisture (RZSM), above-ground biomass (AGB), and snow water equivalent (SWE). The combination of long wavelength and bistatic configuration, which is unique to P-band SoOp methodology, could provide an excellent way to map such geophysical variables globally. To leverage such potential, the development of ground-based testbeds are needed to test and refine both algorithms and forward models. However, its implementation from small Unmanned Aircraft Systems (UAS) platforms is at a relatively low technological readiness level. In this paper, we summarize our efforts on implementing a P-band SoOp receiver from a multi-copter Unmanned Aircraft Systems (UAS) platform. The receiver has gone through several iterations in the lab and field. In this paper, we will provide experimental results as well as the pertinent background and theoretical derivations supporting the design and implementation of the UAS-based instrument.

Index Terms— Signals of Opportunity, P-band, UAS, reflectivity.

1. INTRODUCTION

Root-zone soil moisture (RZSM) is an important variable when forecasting plant growth, determining water availability during drought, and understanding evapotranspiration as a flux [1]. However, current global RZSM estimation methods are indirect and use data assimilation, which requires timeseries data to make model-based predictions [2]. This is because direct measurement requires a lower frequency signal, typically P-band and below (< 500MHz), to reach root-zone depths [3] and, in turn, necessitates a larger antenna to be deployed in space, which is often unfeasible. A new remote sensing technique known as Signals of Opportunity (SoOp) recycles communication signals to perform microwave remote sensing. This means that SoOp platforms need not include a trans-

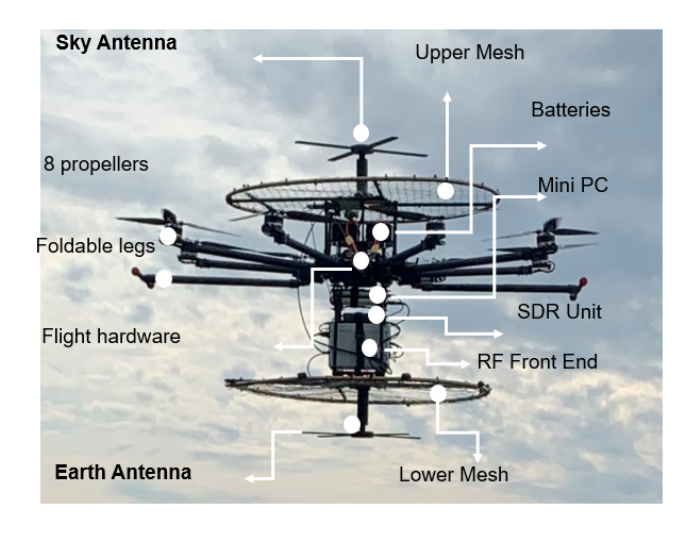


Fig. 1. Octocopter implementation of P-band SoOp receiver.

mitter, but rather rely on passive radar technology to make measurements.

The United States Navy's Mobile Users Objective System (MUOS) at 370 MHz was identified as a candidate satellite system utilizing a lower frequency signal in a SoOp configuration. This signal uses Wideband Code Division Multiple Access (WCDMA) encoding and contains four 5-MHz channels for a total bandwidth of 20 MHz between 360-380 MHz [4]. A custom-built octocopter is used to support the weight (20.8 kg including the UAS) of the receiver system's payload and the size of the attached ground planes as shown in Fig. 1. Each of the components for this UAS were individually sourced to create a purpose-built platform for this application [5]. The receiver payload is greatly influenced by the work done at Radiation Navigation Lab at Purdue University, which implements a tower-based P-band receiver using the same MUOS signal [6]. A similar configuration from a fixedwing UAS has been also studied [7].

Several data collection flights have been conducted with the receiver platform. Each flight performs one of the follow-

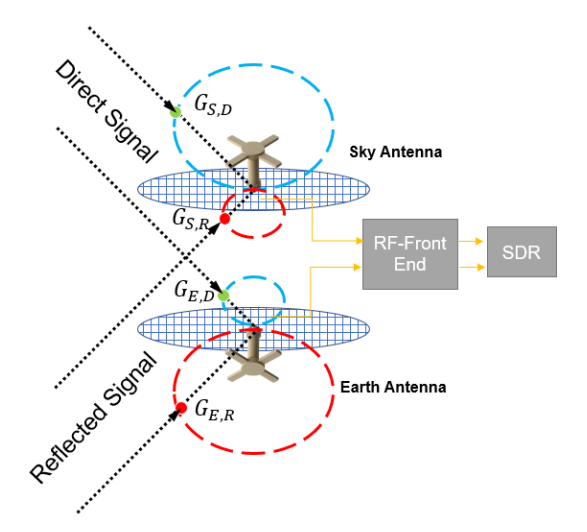


Fig. 2. Measurement configuration. Both direct and reflected signals are routed through RF front end which is followed by software defined radio (SDR).

ing actions: hover over pond, cotton, and corn fields, or movement over pond to crop field and back. In the following sections, the experiments and results will be discussed, and the conclusions and future work are summarized. We will also discuss the pertinent background and theoretical derivations supporting the design and implementation of the UAS-based instrument.

2. METHODOLOGY

A SoOp receiver adheres to a passive bi-static instrument configuration, where both earth-pointing and sky-pointing antennas measure the signal of interest, direct and reflected respectively as illustrated in Fig. 2. Both signals go through a Radio Frequency (RF) chain where the RF front-end employs two approaches to calibrate the channel gains (i.e., antenna swapping through use of a transfer switch, and matched loads). The RF front-end is followed by a two channel software-defined radio (SDR) that synchronously records the radio signals. A short sequence, alternating between the "through" (T), "calibrate" (C) and "swap" (S) states runs continuously, with a few seconds duration of each state set for data collection as well as for noise calibration as illustrated in Fig. 3. Autoand cross- correlation of each channel are combined to produce an estimate of the effective reflection coefficient. Due to longer wavelength, the surface reflection is expected to retain the coherence and dominantly originates at the specular point.

The signals at the earth and sky antennas are delayed and weakened due the path loss and/or reflection when it arrives at each antenna. Under the assumption of good antenna isolation, specular reflection, and far-away transmitter, the reflectivity can be estimated by taking the ratio of signal powers

at the earth to sky antennas [8], i.e,

$$\hat{\Gamma} = \frac{C_R}{C_D} = \frac{G_1 G_{S,D}}{G_2 G_{E,R}} \left(\frac{R_{12}(\tau_{RD})}{R_{11}(0) - G_1 \sigma_1^2} \right)^2 \tag{1}$$

where C_R and C_D is the power of signal along the reflected and direct paths, τ_{RD} is the delay corresponding to the path difference between direct and reflected paths. The quantities G_1 and G_2 are the system gains of each channel while $G_{S,D}$ and $G_{E,R}$ are the antenna gains in the direction of direct path for sky antennas and specular point for earth antenna. The quantity σ_1 is the noise power introduced by channel 1 and used to estimate the noise floor of the receiver. The quantities R_{11} and R_{12} are auto- and cross-correlation functions, respectively.

3. SYSTEM IMPLEMENTATION

The current receiver consists of the following primary subsystems as described in [5]: (1) RF-front end, (2) Universal Software Radio Peripheral (USRP) B210: an SDR for recording radio signals, (2) NUC: an computer communicates with USRP for recording and Pi Zero for state control, (3) Pi Zero: interfaces with RF front end relays for powering and switching states, and (4) Two battery packs: for powering above devices and RF circuitry.

The primary operations of the RF front end are to filter and amplify the received signal and perform the state switching for noise calibration. The front end was first constructed as a ground based receiver in order to become familiar with all the workings of the receiver prior to deployment on a UAS. All components received underwent verification with a vector network analyzer to ensure the component specifications provided by the manufacturer were met. The switching algorithms used to change the states in the receiver were prototyped using a Raspberry Pi to control the mechanical relays linked to the RF components.

Using the lessons learned from building the ground-based receiver, a UAS-based receiver was started. For this implementation, proper planning was required to fit all the same RF and control circuitry into a much smaller package for deployment on the UAS. The enclosure selected was the largest that could fit under the UAS in the payload area, measuring in at 200 mm×200 mm×130 mm (L× W×H). In order to best optimize the space inside, a two layer approach was taken, where the bottom layer in the enclosure would house all the RF components and the top layer would house all the control circuitry, that being the mechanical switches, DC-DC converters, and Raspberry Pi microcontroller. Organizing in this structure also promotes the use of shielding between the RF circuit and the control circuit, which can reduce noise introduced by the mechanical switches and DC-DC converters.

The selected antennas were purchased off-the-shelf and are a pair of Right Hand Circular Polarized (RHCP) and Left

Hand Polarized Circular Polarized (LHCP) antennas designed for mobile deployment with soldiers to communicate with the MUOS satellite constellation. These antennas exhibit an omni-directional radiation pattern, so the antennas will not need to be angled when mounted to receive the signal. Ground planes were designed for both antennas to isolate the UAS electronics and reduce the strength of the unwanted direct signal on the bottom and reflected signal up top. The design is composed of a 91.44 cm diameter metal hoop laced with galvanized steel poultry netting. Poultry netting is used to reduce weight and allow air to flow freely through the ground plane.

An Ettus Research USRP model B210 recorded the radio signals that are amplified by the RF front-end. This model connects to a host computer over the USB3 protocol and enables software tuning of the receiver band. The data is transmitted in real-time over the USB connection, where it is stored on the host computer until offloading to a data storage server.

The Pi runs a Transmission Control Protocol (TCP) server by default that the GNU (GNU's Not Unix) Radio program connects to and instructs when to switch states. Additionally, this enables the ability to note precise timestamps for when the state switching occurs, which provides useful information when processing the data. With this feature added, the GNU radio program is made to record a specific number of samples in each state, rather than basing off of time duration. Additionally, we added an ability to trigger the start of a recording with the UAS controller to improve the data collection process as well. The controller unit on the UAS has General-Purpose Input/Output (GPIO) available that is connected to the Raspberry Pi headers to indicate a recording request and to enable synchronising RF data recording with UAS flight log files.

4. RESULTS

Several data collection flights have now been conducted with the receiver platform. Though some issues were present in initial flights, lessons learned have been applied to the flights carried out afterward, improving data collection results for each flight campaign.

One of the key checks to ensure the receiver is working as intended is the state changes in the peak values of the autocorrelation function. Fig. 3 shows the these values for each channel for one cycle, which is set as 1200 ms. Another key check is presence of two peaks in the cross correlation. Specifically, there should be a peak in the cross correlation of the two channels at the lag that corresponds to the distance in path length between the direct signal and the reflected signal. Fig. 4 displays this relationship.

Finally, one needs to observe the signal in power spectral density (PSD). Fig. 5 displays the PSD of direct channel for the through state and shows four 5 MHz signals bands as expected. This plot is derived from just a single sampling iteration, which runs 1200ms long. The signal shape was not quite

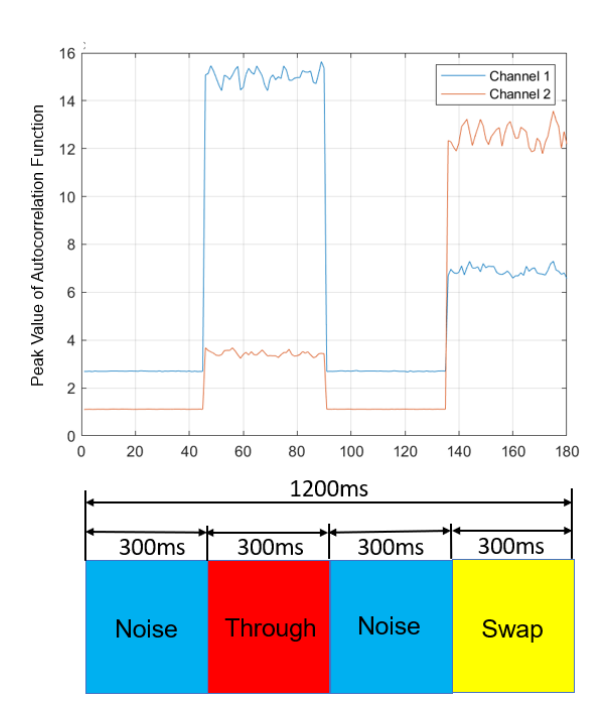


Fig. 3. Peak value of auto-correlation function as a function of measurement sequence.

as obvious in the reflected channel, so further processing and filtering may be required to observe a clear signal in that channel. The issue here does not seem to be RF front end related, the reflected signal appears the same in both the through and swap states, indicating that the RF components are working as intended in both channels.

We have also observed some spikes in the PSD data (see Fig. 5) and we suspect that radio frequency interference or interference between electronics and RF circuitry could be the cause of such spikes. We are currently working on identifying the nature of these spikes and will present our findings in the conference as well.

5. CONCLUSIONS

In this study, we developed a UAS-based P-band SoOp receiver that collects direct and reflected signals transmitted by geosynchronous MUOS satellites for purpose of many earth observation applications including remote sensing of root-zone soil moisture (RZSM), above-ground biomass (AGB), and snow water equivalent (SWE). The RF front end was adapted from the tower-based receiver built by Radio Navigation Laboratory at the Purdue University. We designed and assembled a tightly-packaged front end for drone deployment. We developed in-house software for controlling the SDR and embedded computer as well as scripts for processing raw data collected from the receiver. During the development phase, we investigated the limitations of various SDR models. We

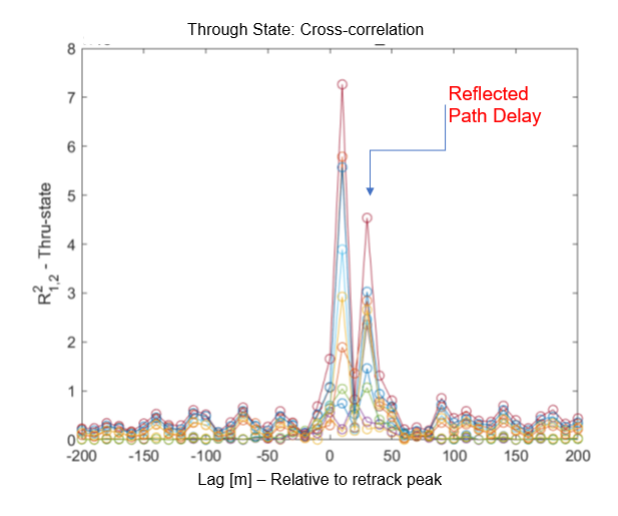


Fig. 4. Peak value of auto-correlation function as a function of measurement sequence. Different colors correspond to processed 20 ms data blocks.

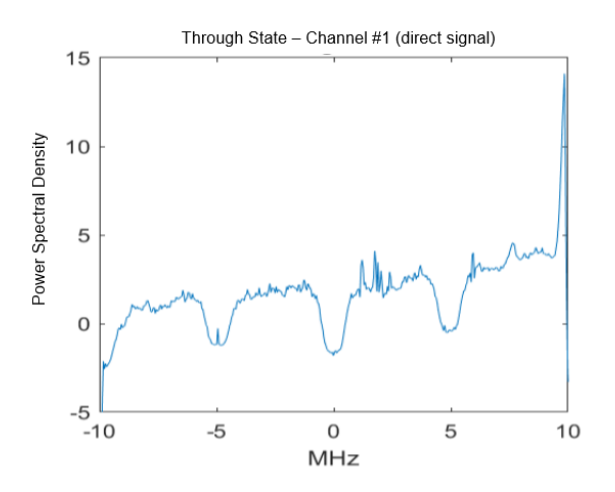


Fig. 5. A sample power spectral density of a direct signal

conducted many tests and data collection flights with no crashes or close calls. These tests helped us to refine the receiver data collection processing steps. The current system proved the functionality of UAS-based P-band receiver platform. However, several improvements are needed for the current system such as the inclusion of temperature sensors into the front-end enclosure for noise calibration. To reduce potential electromagnetic interference between RF circuitry and electronics, implementing higher quality DC-DC converters and solid-state switches are planned. Additionally, we use off-the-shelf amplifier and filters, which are not always noise efficient for our application, so custom filtering and LNA implementation are also planned to remedy saturation from out of band noise. Furthermore, an embedded computer with an integrated battery could help reduce the payload weight and increase the data acquisition efficiency.

6. ACKNOWLEDGEMENT

This work was supported by National Science Foundation (NSF) Grant #2142218.

7. REFERENCES

- [1] E. Babaeian, M. Sadeghi, S. B Jones, C. Montzka, H. Vereecken, and M. Tuller, "Ground, proximal, and satellite remote sensing of soil moisture," *Reviews of Geophysics*, vol. 57, no. 2, pp. 530–616, 2019.
- [2] R. H Reichle, G. JM De Lannoy, Q. Liu, R. D Koster, J. S Kimball, W. T Crow, J. V Ardizzone, P. Chakraborty, D. W Collins, A. L Conaty, et al., "Global assessment of the smap level-4 surface and root-zone soil moisture product using assimilation diagnostics," *Journal of hydrometeorology*, vol. 18, no. 12, pp. 3217–3237, 2017.
- [3] D. R. Boyd, A. C. Gurbuz, M. K., J. L. Garrison, B. R. Nold, J. R Piepmeier, M. Vega, and R. Bindlish, "Cramer–rao lower bound for soop-r-based root-zone soil moisture remote sensing," *IEEE journal of selected topics in applied earth observations and remote sensing*, vol. 13, pp. 6101–6114, 2020.
- [4] J. D Oetting and T. Jen, "The mobile user objective system," *Johns Hopkins APL Technical Digest*, vol. 30, no. 2, pp. 103–112, 2011.
- [5] P. Peranich, "Implementation of uas-based p-band signals of opportunity receiver for root-zone soil moisture retrieval," *MS Thesis, Mississippi State University*, 2021.
- [6] J. L Garrison, M. Kurum, B. Nold, J. Piepmeier, M. A. Vega, R. Bindlish, and G. Pignotti, "Remote sensing of root-zone soil moisture using i-and p-band signals of opportunity: Instrument validation studies," in *IGARSS* 2018-2018 IEEE International Geoscience and Remote Sensing Symposium. IEEE, 2018, pp. 8305–8308.
- [7] S. Yueh, R. Shah, X. Xu, K. Elder, S. Margulis, G. Liston, M. Durand, C. Derksen, and J. Elston, "Uas-based pband signals of opportunity for remote sensing of snow and root zone soil moisture," in *Sensors, Systems, and Next-Generation Satellites XXII*. International Society for Optics and Photonics, 2018, vol. 10785, p. 107850B.
- [8] J. Garrison, Y.C. Lin, B. Nold, J. R. Piepmeier, M. A. Vega, M. Fritts, C. F. Du Toit, and J. Knuble, "Remote sensing of soil moisture using p-band signals of opportunity (soop): Initial results," in 2017 IEEE International Geoscience and Remote Sensing Symposium (IGARSS). IEEE, 2017, pp. 4158–4161.